



Cite this: *Nanoscale Adv.*, 2019, **1**, 2801

## Recent advances in the use of $\text{TiO}_2$ nanotube powder in biological, environmental, and energy applications

Walaa A. Abbas, Ibrahim H. Abdullah, Basant A. Ali,  Nashaat Ahmed, Aya M. Mohamed, Marwan Y. Rezk, Noha Ismail, Mona A. Mohamed  and Nageh K. Allam \*

Received 29th May 2019  
Accepted 1st July 2019

DOI: 10.1039/c9na00339h  
[rsc.li/nanoscale-advances](http://rsc.li/nanoscale-advances)

### Introduction

Nanomaterials with a tubular morphology enjoy unique properties over other morphologies, making them the target for many applications. Therefore, a plethora of fabrication techniques have been demonstrated in the literature to synthesize such nanotubes from different materials. Specifically, huge interest has been shown in the synthesis of titania nanotubes and their applications due to their biocompatibility,<sup>1–3</sup> antimicrobial properties,<sup>4,5</sup> high chemical stability, specific surface area, and catalytic activity.<sup>6–8</sup> In addition, the high UV

absorption and the possibility to modify the band gap promote titania as a good candidate for photocatalysis, making it useful for producing sunscreen materials<sup>9</sup> and in water treatment.<sup>10–13</sup> Of special interest, titania nanotubes in the powder form (TNTP) have recently gained great interest within the scientific community. To this end, many synthesis methods have been established to fabricate TNTP as shown in Fig. 1, including ultra-sonication after anodization, rapid breakdown anodization, and hydrothermal techniques. In this mini-review, the properties of TNTP will be highlighted by giving insights into their different synthesis techniques and use in a plethora of applications.

### Fabrication methods of TNTP

There are two main approaches to fabricate  $\text{TiO}_2$  nanotubes in the powder form as presented in Scheme 1. The first approach is the anodization of Ti foil, which can be subdivided into two techniques. While the first approach includes the anodization of Ti foil followed by controlled ultrasonication,<sup>14</sup> the second technique is a one-step process known as rapid breakdown



Nageh Allam received his Ph.D. degree from Pennsylvania State University in Materials Science and Engineering. He joined the Georgia Institute of Technology as a postdoctoral fellow and then the Massachusetts Institute of Technology as a research scholar. He moved to The American University in Cairo in September 2011 where he is now a professor of Materials Science and Engineering. His research focuses on

the fabrication of well-designed nanostructured materials with composition, size and shape control for use in energy conversion and storage, sensor applications, and biomedical applications, among others. His research comprises both experimental and theoretical activities.

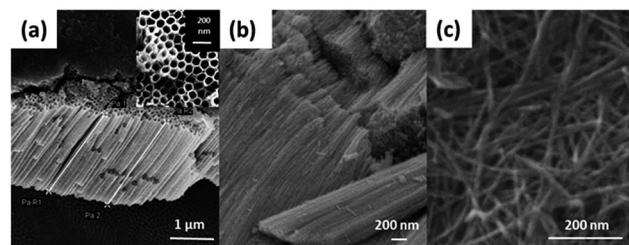
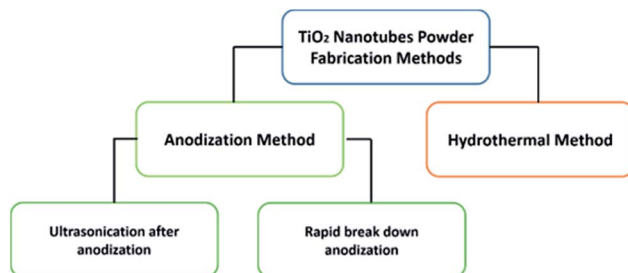


Fig. 1 FESEM images of TNTP prepared by the authors via (a) ultrasonication, (b) rapid breakdown anodization, and (c) hydrothermal techniques.





Scheme 1 Fabrication methods of titania nanotubes in the powder form.

anodization.<sup>15,16</sup> The second approach is the hydrothermal synthesis of TNTP.<sup>17,18</sup> Although there are other methods for producing tubular titania such as sol-gel and template-based synthesis methods,<sup>19–21</sup> they are not commonly used.

## Anodization technique

The anodization process, a top-down fabrication technique, is an electrochemical method that produces an oxide layer on the surface of metals.<sup>22</sup> In order to achieve the tubular array formation, there are three main processes: the first process is the field assisted oxidation of titanium metal to produce an oxide layer on its surface and to form TiO<sub>2</sub>. The second is the field assisted dissolution of titanium metal ions in the electrolyte. The final one is the surface etching resulting from the chemical dissolution of titanium and TiO<sub>2</sub> as shown in Fig. 2.<sup>3,19,23,24</sup> Extensive research studies have investigated the factors that govern the nanotube formation with tuned tube diameter and length.<sup>25–29</sup> The formed oxide layer structure on the metal surface mainly depends on the concentration and composition of the electrolyte solution and the applied voltage.<sup>5,8</sup> The effect of the electrolyte composition on the length of titania nanotubes is summarized in Fig. 3.

It has been reported that the formation of highly oriented TiO<sub>2</sub> nanotubes with lengths  $\approx 500$  nm is achieved by the use of HF acidic aqueous electrolyte in the anodization of the titanium metal.<sup>30</sup> Many researchers have paid attention to further synthesis approaches to enhance the titanium tube length and reduce the dissolution of the oxide layer on the surface of the Ti metal in a robust acidic medium. Therefore, several studies have been conducted to replace acidic HF electrolyte with fluoride salts such as NH<sub>4</sub>F, NaF, and KF at adjusted pH in order to increase the titanium nanotube length up to 6  $\mu\text{m}$ .<sup>31–37</sup> A novel approach was used to fabricate highly oriented titania nanotubes with a long tube length that reached up to 720  $\mu\text{m}$ .

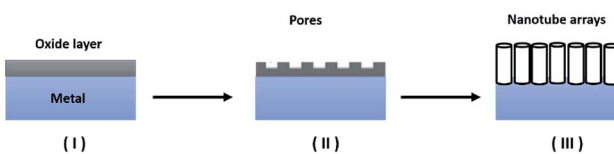


Fig. 2 A schematic diagram of nanotube formation by anodization.

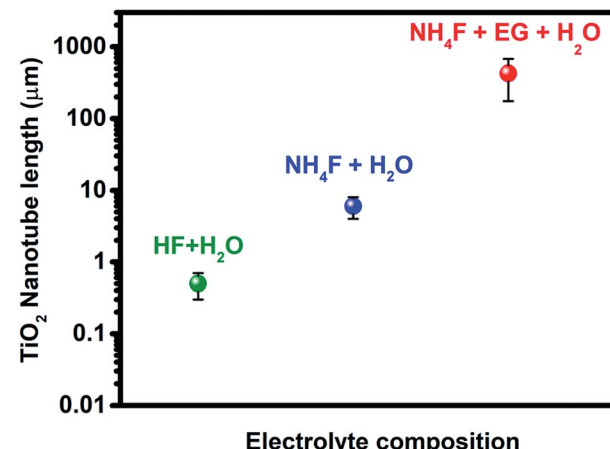


Fig. 3 Effect of the electrolyte composition on the length of titania nanotubes formed during anodization.

using the combination of non-aqueous organic electrolytes such as ethylene glycol (EG) or formamide (FA) with HF, KF, NaF, and NH<sub>4</sub>F.<sup>19,30,32–37</sup>

### Anodization and ultrasonication

Following the anodization of Ti foil, the TNTP can be formed *via* ultra-sonication of the pre-grown titania nanotubes followed by repetitive anodization and ultra-sonication processes until all the Ti foil has been fully converted into aligned nanotube powder. This process is also known as two-step anodization because the metal foil is used, recycled until it is fully consumed and converted into fine tubular powder.<sup>14</sup>

Although this method produces high surface area and well-defined structures of TiO<sub>2</sub> tubular arrays, it has several drawbacks. In fact, it is considered time-consuming to extract the tubes and recycle the metal foil with an extremely small yield of the powder *via* ultra-sonication. In other words, the electrochemical reaction takes 2 hours per one  $\text{cm}^2$  of foil to produce only 0.01 g after annealing at 450 °C. In addition, due to the increase in temperature during ultra-sonication, the titania tubular architecture might be collapsed. Furthermore, the tubes are usually contaminated by electrolyte impurities, which could negatively affect their properties.<sup>14</sup>

### Rapid breakdown anodization

Using the rapid breakdown anodization technique to produce TNTP is considered the simplest and most cost-effective approach because it provides a high yield and can be achieved through a single electrochemical anodization step. The produced TNTP can be easily used in different applications due to their high surface area and aspect ratio. As discussed before, the formation mechanism of TNTP is mainly attributed to the chemical oxidation and dissolution of the metal substrate. In the rapid breakdown anodization, chloride ions are mainly used instead of fluoride ions in the electrolyte (e.g. perchloric acid).<sup>14</sup> During the initial phase, the oxide layer is formed through the hydrolysis of the titanium metal surface. Once an electric field is



applied, migration and transport of ions occur through the dissolution process, where  $\text{Ti}^{4+}$  cations migrate toward the electrolyte solution, and *via* the oxidation process, where oxygen anions diffuse towards the metal/oxide interface forming a thick oxide layer. After that, the electrolyte resistance is increased causing the anodic oxidation to stop. Then, the chloride anions start to dissolve the metal oxide layer forming pores which resulted from the localized breakdown of the oxide interface. The titanium dioxide white layer leaves the substrate and breaks down gradually in one dimension developing vertically oriented nanotubes in the electrolyte in the powder form as indicated by eqn (1)–(4).<sup>15,16,38</sup>



The chemical interactions explained above occur due to the mechanical stress established at the  $\text{Ti}/\text{TiO}_2$  interface. Moreover, the strong chemical reactions between the Ti substrate and chloride ions cause hydrogen evolution at the Pt electrode.<sup>15,16</sup> A comparison between ultra-sonication, rapid breakdown anodization, and hydrothermal techniques is summarized in Table 1.<sup>15,16</sup> Fig. 4 summarizes the factors controlling the formation of TNTP such as the applied voltage, type and concentration of the electrolyte, temperature, pH, and fabrication processing period that definitely affects the tube diameter, tube length, etching rate, homogeneity, and roughness.<sup>29</sup>

### Hydrothermal processing

The hydrothermal process is used for crystal formation and growth.<sup>39</sup> It is considered the most commonly used technique for the synthesis of TNTP due to its simplicity and high yield. Typically, amorphous TNTs are treated at high temperature in

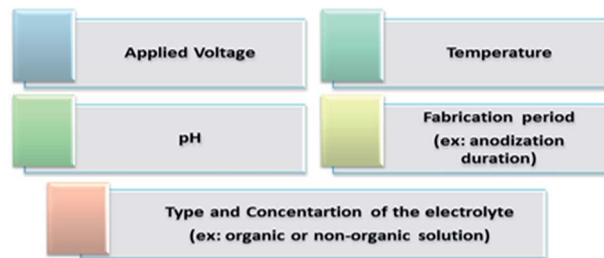


Fig. 4 Factors affecting TNTP formation.

a concentrated sodium hydroxide solution.<sup>40,41</sup> According to Moazeni *et al.*<sup>42</sup> the formation of TNTP *via* hydrothermal processing involves six main steps. Initially,  $\text{TiO}_2$  and NaOH are mixed and stirred for 1 h and then subjected to ultra-sonication for another hour. The obtained suspension is then transferred to a Teflon-lined autoclave to be heated for 2 days. The resulting powder is washed and then aged in HCl to reach pH 2. The powder is then washed several times with deionized water and ethanol and dried at 40 °C for one whole day. It was noted that the alkaline solution caused some of the Ti and O bonds to be broken to form lamellar fragments as the growth mechanism was attributed to slow dissolution of  $\text{TiO}_2$  in a highly concentrated alkali solution. As titanate ions react with sodium from the alkali solution, they merge to form layered nanosheets. The induced mechanical stress caused by titanate ions at the borders of the sheets makes them scroll and wrap in the form of tubes.<sup>42</sup> Zeng *et al.*<sup>43</sup> used a similar technique to produce powder nanotubes. However, instead of treating  $\text{TiO}_2$  with NaOH at room temperature and stirring, they used NaOH solution inside a Teflon-lined autoclave at elevated temperature for 24 h. Upon subsequent cooling of the solution, it was titrated to reach the desired pH and dried. The obtained nanotubes have an outer diameter less than 10 nm and length less than 1  $\mu\text{m}$ .<sup>43</sup> Zavala *et al.*<sup>39</sup> investigated the effect of hydrothermal treatment, annealing temperature, and acid washing on the morphology of  $\text{TiO}_2$  nanotubes. They realized that the hydrothermal treatment alters the  $\text{TiO}_2$  from the

Table 1 Comparison between the three main techniques for producing  $\text{TiO}_2$  nanotube powder (TNTP)

	Ultra-sonication technique	Rapid breakdown anodization	Hydrothermal technique
Advantages	Produces aligned nanotube arrays  High surface area Cost-effective	Produces dispersed crystalline $\text{TiO}_2$ NTs  High surface area Cost-effective High yield in a few minutes Need to rinse with DI water to ensure that $\text{TiO}_2$ nanotubes are free of electrolyte impurities	Produces highly pure randomly aligned $\text{TiO}_2$ NTs High surface area Cost-effective High yield Applicable on a large scale Time-consuming (long processing time) Chemical-consuming Produces non-uniform TNTs Short length by default
Drawbacks	Under any circumstances, the tubular structure may collapse leading to reduced surface area Very low yield (0.01 g for 1 $\text{cm}^2$ of foil) Time-consuming  Repetitive and risky process, due to its two steps Electrolyte may contain impurities that adversely influence the biological applications		



anatase to monoclinic phase. In addition, the temperature range between 400 °C and 600 °C maintained a highly stable tubular structure. Increasing the temperature above 600 °C resulted in the formation of irregular nanoparticles that are larger than the precursor TiO<sub>2</sub> particle size. Moreover, the crystalline phase was changed from anatase to rutile. Finally, they proved the importance of acid washing as the exchange of Na<sup>+</sup> ions promoted the formation of highly pure nanotubes.<sup>18,39</sup> The hydrothermal processing is considered a relatively cost-effective method that produces highly pure TiO<sub>2</sub> nanotubes. However, some drawbacks of the method should be taken into consideration, including non-uniformity, short length, and long synthesis time. However, it was shown that sonication pre-treatment would aid in increasing the length of the resulting nanotubes.<sup>44</sup> Also, the stirring revolving speed was manipulated as a mechanical force to enhance the diffusion and the reaction rate of TiO<sub>2</sub> nanocrystals to produce longer TNTP.<sup>45,46</sup>

## Applications of TNTP

Although TiO<sub>2</sub> nanotubes in the powder form have been used in many applications, this review is focused on the specific applications shown in Fig. 5.

## Biological applications

### Drug delivery applications

TiO<sub>2</sub> nanotubes have been recently utilized to address the shortcomings of the conventional drug therapeutic solutions, particularly due to the excellent physicochemical properties and biocompatibility they possess.<sup>3</sup> As current drug therapies may suffer from short circulating time, tedious pharmacodynamics, low resistance to the gastrointestinal system, and limited drug solubility, TNTP can help by providing an innovative delivery route for drugs to reach their target sites.<sup>47</sup> It is worth noting that the diffusion process of TNTP when implanted in the body is governed by Fick's first law. This indicates that the drug

release process will be dependent on several elements such as the nanotubes' charge, dimensions, and surface chemistry, and the loaded drug's charge, molecular size, and diffusion coefficient, as well as the type of interaction between the drug molecules and TiO<sub>2</sub> inner surface, see Fig. 6.<sup>48,49</sup> Accordingly, controlling the drug release profile is expected to depend on the fabrication and implementation conditions of TNTP. It is also of importance to mention that the most common drug release strategy is of the zero-order type, in which the release rate is constant regardless of the duration.<sup>48</sup> In this regard, several studies tried to modify the nanotubular structure to suit the desired therapeutic strategy. These modifications include the adjustment of their length, thickness, pore opening, or stimulating their releasing process by polymeric coatings or other external sources.<sup>50,51</sup> For instance, Aw *et al.* found that extending the tubular length from 25 to 100 μm resulted in an increase in the release duration for TiO<sub>2</sub> nanotube drug delivery implants.<sup>52</sup> Other types of drug release strategies consider varying dynamic change of the release kinetics, improving the drug loading and release patterns, multi-drug release, *etc.*, which were all pursued in numerous studies through functionalization of the nanotubular surface.<sup>53,54</sup> For example, TiO<sub>2</sub> nanotubes functionalized with 2-carboxyethyl-phosphonic acid and organic silanes such as penta-fluorophenyl dimethyl chlorosilane and 3-amino-propyl triethoxysilane have been utilized to modify the kinetics of both drug loading and release. This was obtained by changing the hydrophilic and hydrophobic properties of the nanotubular surface, which altered the interaction mechanism between the loaded drug and its carrier, the functionalized TiO<sub>2</sub> nanotubes.<sup>55</sup> For better controlled and sustained release profiles, several studies have reported exposing TiO<sub>2</sub> nanotubes to external triggers such as ultrasound waves, radiofrequency,

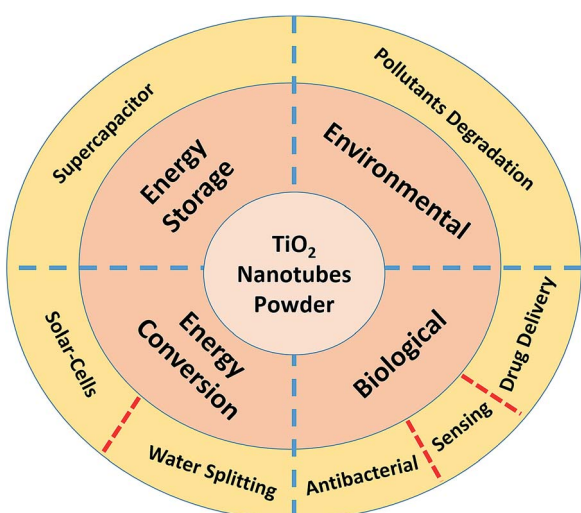


Fig. 5 Selected TNTP applications.

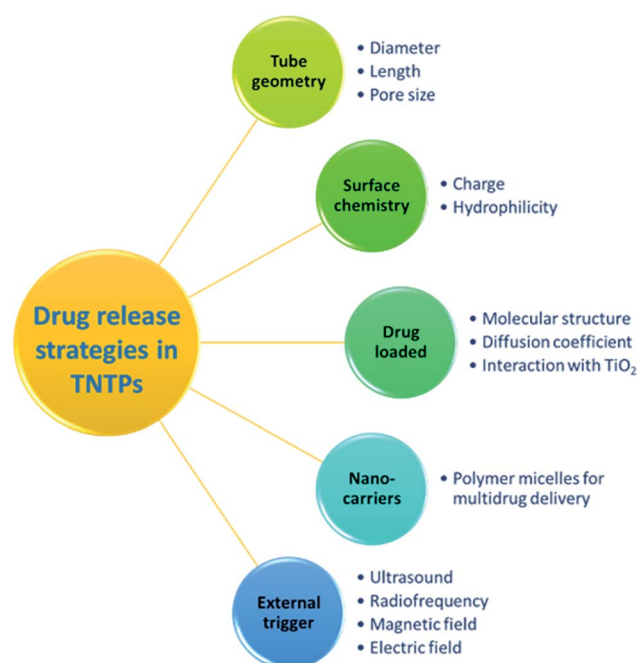


Fig. 6 Governing strategies of drug release profiles using TNTP.



magnetic fields, and electric fields.<sup>56</sup> As an example, the concept of ultrasound-sensitive systems of drug delivery has been proved by Aw *et al.* using  $\text{TiO}_2$  nanotubes. The drug-micelle release profile has shown a promising chance to be enhanced in accordance with the power intensity, pulse amplitude, length, and duration. This may be attributed to the combination of both cavitation and thermal processes triggered by ultrasonic waves. Accordingly, a better interaction between the loaded drug and  $\text{TiO}_2$  nanotubes is expected.<sup>57</sup> This sort of modification would be of significant importance in local and complex delivery systems such as in brain and stent applications. Regarding the cytotoxicity effect of anodized  $\text{TiO}_2$  nanotubes on different types of cells, Li *et al.*<sup>58</sup> have argued that the cytotoxicity of different nanostructures relies on their physicochemical factors such as size, shape, dose, surface charge, and chemical composition. In fact, the three main factors that influence the use of metal oxides in biomedical applications are size, shape, and dose.<sup>58</sup> Chassot *et al.*<sup>59</sup> performed a study to test the cytotoxicity of  $\text{TiO}_2$  nanotubes fabricated *via* the anodization method using protozoan *T. pyriformis* cells for *in vitro* studies. The research did not observe any cytotoxicity and confirmed that  $\text{TiO}_2$  nanotubes are not toxic.<sup>59</sup> However, with all these possibilities and remarkable potential of  $\text{TiO}_2$  nanotube powder to be used in drug delivery systems, further *ex vivo* and *in vivo* animal studies are needed to examine the long-term tolerability and cytotoxicity of the material.

### Antibacterial applications

Remarkable attention has been paid to the use of  $\text{TiO}_2$  nano-materials in the field of photocatalytic bacterial disinfection.<sup>60,61</sup> TNTP, as nanostructured semiconductor materials, are potent photoactive catalysts. They were utilized for eradicating harmful microorganisms and bacteria from water using solar irradiation.<sup>62</sup> Using its different morphologies on the nano-scale,  $\text{TiO}_2$  has been proven to possess several advantages such as superior antimicrobial activity, high photo-stability (high corrosion resistance), biocompatibility, and strong photochemical oxidative activity. All these properties have qualified  $\text{TiO}_2$  as an excellent material for water microbial purification.<sup>63</sup> Basically, the mechanism of water disinfection by TNTP relies on the hydroxylation reactions that start with the formation of hydroxyl radicals ( $\text{OH}^\cdot$ ). Upon light absorption by TNTP, the created electron-hole pairs trigger electrochemical redox reactions which produce free radicals such as hydroxyl radicals ( $\text{OH}^\cdot$ ).<sup>64</sup> In the aqueous medium, these active radicals are strong enough to destroy the bacterial cell wall along with different other cellular components with extremely low survival levels as shown in Fig. 7.<sup>65</sup> Typically, these  $\text{OH}^\cdot$  radicals are produced by the reactions of holes with either  $\text{H}_2\text{O}$  molecules, their hydrolysed  $\text{OH}^-$  ions, or even bacterial membrane lipids.<sup>66</sup> The radicals cause some deleterious effects on the extracellular medium of the bacteria, leading to serious chemical/biomolecular transformations. On the other hand, the electron counterparts combine with the proton ions ( $\text{H}^+$ ) in the same physiological environment to complete the other half of the electrochemical reaction.<sup>67,68</sup>

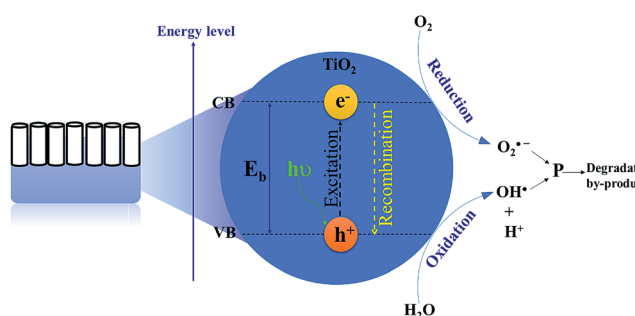


Fig. 7 The principal mechanism for using TNTP in the process of water microbial disinfection.

The effect of the concentration of titania in the lysogeny broth (LB) nutrient medium was tested against bacterial growth in drain water. The study by Carroll *et al.*<sup>69</sup> has concluded that titania powder has the ability to diminish the growth of bacterial colonies even under dark conditions, with a reverse proportionality between the bacterial growth rate and the titania powder concentration.<sup>69</sup> Interestingly, Abbas *et al.*<sup>70</sup> have studied how different types of TNTP can deactivate the growth of *Escherichia coli* (*E. coli*) in contaminated water. The TNTP studied were prepared by both hydrothermal and rapid breakdown anodization techniques, along with other titania structures. The study has revealed that the hydrothermally synthesized TNTP were the best among other titania nano-structures, resulting in the highest inactivation rate of the *E. coli* bacteria under both dark and light conditions for 120 min.<sup>70</sup> It was suggested that the hydrothermally prepared TNTP have a high abundance of  $-\text{OH}$  functional groups on their surfaces, mixed rutile and anatase phases, and remarkably high surface area. All these factors offered this particular structure the highest potential to result in the highest efficacy against bacterial growth in wastewater.<sup>70</sup>

## Energy conversion applications

### Solar cell applications

The vast majority of commercially available solar cells are made from silicon with different solid state junctions. The overall conversion efficiency is varied according to whether the silicon is mono- or multi-crystalline. Several approaches are being explored now in an attempt to achieve higher efficiencies with cost-effective materials. A promising photoelectrochemical concept is utilizing dye-sensitized  $\text{TiO}_2$  solar cells. In 1985, a Ru-based dye was adsorbed on  $\text{TiO}_2$  nanoparticles, which allowed the conversion of solar energy to electricity with 80% quantum efficiency.<sup>71</sup> Later on, Grätzel implemented the concept to fabricate a full dye-sensitized solar cell (DSSC).<sup>72</sup> The classic DSSC is mainly made of  $\text{TiO}_2$  crystalline nanoparticles attached to a conductive substrate, a Ru-based dye as a sensitizer, an electrolyte, and platinum as a counter electrode.<sup>73</sup> A fundamental aspect of dye selection is that the LUMO of the dye has to be energetically higher than the  $\text{TiO}_2$  conduction band. Upon exposure to sunlight, the excited electrons of the dye are



injected from the LUMO into the semiconductor's conduction band (see Fig. 8). The dye gets reduced through the redox reaction catalyzed by the electrolyte. The electrolyte is either an ionic liquid or an organic solvent. In addition to the crucial thermodynamic considerations, reaction kinetics have to be fulfilled, the electron injection from the semiconductor conduction band has to be faster than dye de-excitation, and also the dye regeneration time constant has to be fast enough to minimize any depletion effects.<sup>74,75</sup> The struggle between effective electron transport within  $\text{TiO}_2$  and electron recombination possibilities is a limiting factor. Generally,  $\text{TiO}_2$  nanoparticles suffer from slow transport time constants owing to trapping/de-trapping effects. The hindered diffusion coefficient of the  $\text{TiO}_2$  nanoparticles is due to grain boundaries, defects, surface states, *etc.*, which drastically contribute to diminished electron flow as they act as trapping sites.<sup>76,77</sup> In this regard, one-dimensional nanostructures such as TNTP can significantly improve the overall electron transport mechanism owing to limited inter-crystalline traps that lower the possibility of recombination. However, although many types of solar cells have been produced using 1D  $\text{TiO}_2$  morphologies, the multidirectional orientations of the misaligned 1D nanostructures do not guarantee the best unidirectional flow of electrons along the longitudinal length. The perfect 1D nanostructures provide rapid, conductive electron transport and the orientation becomes less important. This may apply for single crystalline nanostructures free from defects. Current approaches tend to grow polycrystalline  $\text{TiO}_2$  nanotubes, where a vertical alignment can compromise between electron transport and charge efficiency. Anodic oxidation approaches for synthesis of self-assembled titania nanotubes are becoming of great interest.<sup>78,79</sup>

The sole role of  $\text{TiO}_2$  in DSSCs is to harvest the injected electrons from the dye. Although other oxides could be considered as an alternative, until now  $\text{TiO}_2$  is the best choice. TNTPs synthesized *via* rapid breakdown anodization (RBA) lead to the formation of flower-like bundles with very high aspect ratios when using perchlorate or chloride electrolytes. These TNTP show excellent performance in DSSCs.<sup>80</sup> The  $\text{TiO}_2$  DSSC performance is mainly dictated by the degree of crystallinity. Upon elevating the temperature, the rutile phase dominates with the possibility of collapse. Thus, anatase is the phase of

choice for efficient titanium-based solar cells as it is the most photoactive phase. Different groups have already reported several results but it is hard to compare these results because the overall produced efficiency is dictated by not only the intrinsic properties of the  $\text{TiO}_2$  NTs but also the entire solar cell structure *i.e.* the actually investigated active area within the solar cell, the distance between the nanotubes, and the counter electrode.<sup>81</sup>

The effects of combining TNTP and  $\text{TiO}_2$  nanoparticles prepared *via* sol-gel and hydrothermal methods, respectively, have been studied through measuring the performance of the solar cell. Various weight ratios of the TNTP and  $\text{TiO}_2$  nanoparticles were mixed together. The open TNTP structure facilitated better penetration of the electrolyte and enhanced the contact between the dye, tubes, and electrolyte. The high surface area of the nanotubes and the nanoparticles enhanced the amount of adsorbed dye. The crystal properties of the anatase phase were found to be the best at a hydrothermal temperature of 150 °C for 12 h. The overall conversion efficiency of the DSSC reached 4.56% under AM 1.5 illumination. It is worth mentioning that the photovoltaic performance of the DSSC made of hybrid titania nanoparticles and nanotubes is enhanced compared to that of the DSSC made purely of  $\text{TiO}_2$  nanoparticles.<sup>82</sup> Also, the hybrid nanotubes and nanoparticles were tested in perovskite solar cells (PSCs). A  $(\text{CH}_3\text{NH}_3)_2\text{PbI}_3$  PSC based on  $\text{TiO}_2$  nanotube and nanoparticle hybrid photo-anode was successfully constructed without affecting the nanotubular structure. The charge efficiency was maximized and the recombination rates were suppressed. In this assembled device, the nanotubes boosted the light scattering and hence absorption by the sensitizer. The nanoparticles enhanced the adhesion of the cell components. Using carbon as a counter electrode, the conversion efficiency of the PSC reached 9.16% under 1.5 AM illumination.<sup>83</sup> Hydrothermally annealed TNTP were sensitized with poly[2-methoxy-5-(2-ethylhexyloxy)-1,4-phenylenevinylene] (MEHPPV) as a conducting polymer used to improve the donor-acceptor mechanism of the hybrid solar cell. The different thermal treatments of the  $\text{TiO}_2$  nanotubes revealed drastic morphological, structural, electrical and optical alterations of the nanotubes, in addition to the remarkable induction of crystallinity and hence charge transfer enhancement. Here, the nanotubes act as an acceptor material and the MEHPPV polymer acts as a donor material, which improved the energy conversion of the organic solar cell.<sup>84</sup> In an attempt to study the effect of different sensitizers on the efficiency of the TNTP, zinc porphyrin-imide dye was adsorbed on the  $\text{TiO}_2$  nanotubes by immersion for 24 h. The absorption spectra of the used zinc porphyrin-imide dye are usually seen at 439 nm and 620 nm. Upon adsorption on the  $\text{TiO}_2$  nanotubes, the peaks were shifted to 421 nm and 640 nm. The assembled DSSC showed a conversion efficiency of 1.914% from the front side and 1.147% from the backside.<sup>85</sup>

### Photocatalytic water splitting

Environmental pollution and depletion of fossil fuels have become serious issues. In this regard, numerous studies have

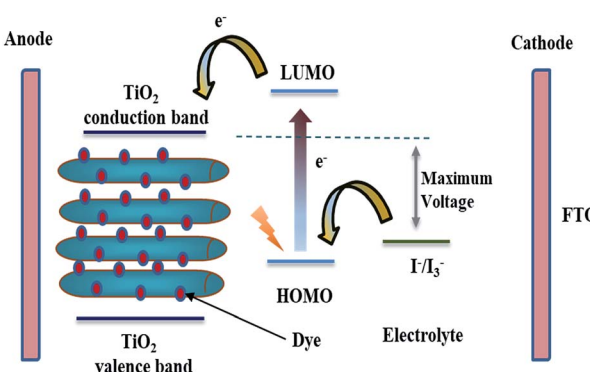


Fig. 8 Schematic diagram of a DSSC using TNTP as an anode.



been carried out to utilize a renewable energy source that should be as efficient as fossil fuels but pollutant free. Harvesting solar energy has been utilized in photocatalytic hydrogen production *via* water splitting.<sup>86</sup> Photocatalytic processes are reactions that can be accelerated or activated by means of the absorption of photons.<sup>87</sup> Absorbed photons yield photogenerated electron/hole pairs that can derive certain redox reactions such as degradation of organic pollutants and water splitting. Among the photocatalytic materials, semiconductors are of great interest due to their potential applications in solar energy harvesting. However, for a semiconductor to allow a certain photocatalytic reaction, it must satisfy some criteria including a relatively small band gap to harvest as much energy as possible from the solar spectrum and convert these photons to well-separated charge carriers ( $e^-/h^+$  pairs).<sup>88,89</sup> It also needs to exhibit high chemical stability in aqueous electrolytes as well as being earth abundant to be cost-effective. Fig. 9 illustrates the conditions that should be satisfied by a semiconducting material for use in solar water splitting.<sup>88</sup>

In this regard,  $TiO_2$  has been considered as an outstanding photocatalyst owing to its high chemical stability, availability, low cost, and environmentally friendly nature. Despite all these advantages,  $TiO_2$  suffers from its restricted absorbance in the UV region of the solar spectrum as well as the fast recombination rate of the photogenerated charge carriers.<sup>90,91</sup> In order to overcome these drawbacks, the morphology of  $TiO_2$  was modified to obtain one dimensional  $TiO_2$  nanotubes that can offer an enhanced photocatalytic performance due to the enhanced separation of photogenerated charge carriers by decoupling the direction of light absorption and charge carrier collection.<sup>92</sup> Moreover, band gap engineering *via* doping, decoration and/or alloying with different elements (metals or non-metals) was reported to extend its light harvesting into the visible region of the solar spectrum.<sup>93,94</sup>

David *et al.*<sup>95</sup> reported the impact of loading TNTs, fabricated *via* rapid breakdown anodization, with Pt, Pd and Ni nanoparticles on the efficiency of hydrogen generation *via* solar water splitting. The as-prepared TNTs were annealed at 450 °C for 3 h then sensitized with the metal nanoparticles through the chemical reduction approach using  $NaBH_4$ . The XRD patterns showed that all the samples exhibited a pure anatase phase

without any induced crystal structure modification. The metal nanoparticles were loaded on TNTs with two different concentrations, 5 wt% (denoted as PtA, PdA and NiA) and 10 wt% (denoted as PtB, PdB and NiB). The samples loaded with Pt and Pd nanoparticles exhibited enhanced hydrogen generation due to the created Fermi level of the metal just beneath the conduction band of the TNTs, resulting in an increased life time for the photogenerated charge carriers to drive the corresponding water splitting process. At high concentration of metal NP loading, the samples showed a decreased photocatalytic performance due to the agglomeration of the metal NPs at the active sites of the TNTs, thus preventing the penetration of light to these sites. On the other hand, sensitizing the TNTs resulted in deterioration of the hydrogen generation rate of the Ni sensitized TNTs compared to the pristine one. This behaviour was attributed to the created impurity level, which was far below the CB of the TNTs, making it difficult for the photogenerated electrons in the CB to be transferred to the Fermi level of the Ni NPs.<sup>95</sup>

For non-metal doping, Preethi *et al.* showed that N-doped triphase (anatase-rutile-brookite) TNTP exhibited a superior photocatalytic activity for solar water splitting compared to the pristine triphase TNTs. This enhancement was ascribed to engineering the band gap by N-doping from 3.06 eV down to 2.87 eV, which resulted in extending the photocatalytic activity into the visible region of the solar spectrum as illustrated by the charge transfer mechanism shown in Fig. 10. The pristine triphase TNTP was prepared *via* the rapid breakdown anodization method. While the N-doped sample was prepared by adding different concentrations of hydrazine hydrate to the electrolyte solution rather than annealing the pristine  $TiO_2$  in an  $NH_3$  atmosphere since annealing in an  $NH_3$  atmosphere resulted in the formation of N-doped biphasic TNTs. The XRD patterns confirmed that both pristine and N-doped TNTP exhibited diffraction peaks that are indexed to the three phases (anatase-rutile-brookite). Also, it was illustrated that increasing the concentration of the N dopant induced phase transformation

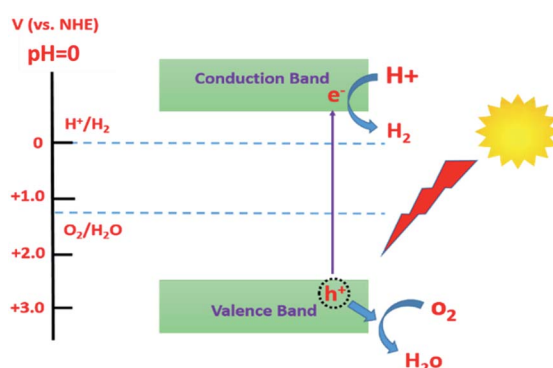


Fig. 9 Semiconductor requirements for solar water splitting.

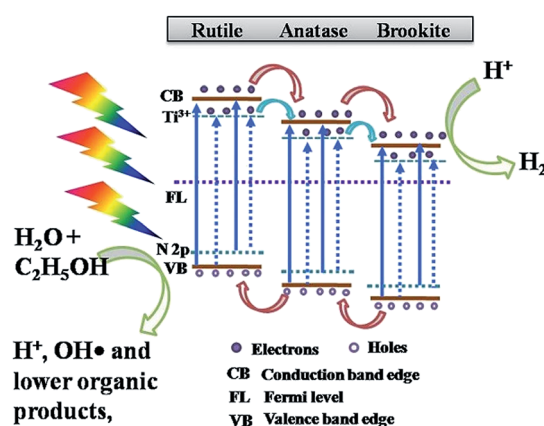


Fig. 10 Schematic diagram of the charge transfer mechanism in 0.29 atomic% N-doped triphase TNTP. Reproduced from ref. 94 with permission from the Nature Publishing group under Creative Commons Attribution 4.0 International License.



from brookite to anatase. The photocatalytic measurements revealed that doping  $\text{TiO}_2$  with a nitrogen concentration of 0.29 atomic percentage exhibited the best photocatalytic performance in hydrogen production ( $30.2 \text{ mmol g}^{-1}$ ) via solar water splitting.<sup>94</sup>

## Energy storage applications

Due to the increased need for energy in our daily life, it is mandatory to fabricate long-lasting energy storage devices. In this regard, supercapacitors are considered the energy storage devices of the future. Electrochemical capacitors (EC) can store energy in the form of electrical charges.<sup>96</sup> The materials used for supercapacitors can be divided into three main categories.<sup>97-99</sup> First, materials that store energy in the form of electric double layers (EDLs), which are mainly carbon allotropes such as graphite, graphene, and carbon nanotubes. Second, materials that store energy through a fast-redox reaction from different chemical groups such as oxides, sulfides, nitrides, or conducting polymers.<sup>100,101</sup> Third, composite materials of both active and double layer materials.<sup>96,99</sup> In battery-like materials, the capacitance is subject to change over the potential window.<sup>102</sup> The process of storing energy through a redox reaction is usually referred to as the "faradaic process". In the faradaic process, a fast reversible redox reaction occurs at the surface of the electrode material resulting in adsorption of electrolyte ions and exchange of electron charges between the electrolyte and the electrode material.<sup>96,103</sup> The surface of the material is the main factor that controls the adsorption of the ions and the charge exchange. Thus, the morphology of the material is a good subject to be studied as it affects the mechanism and the quality of the pseudocapacitor material.<sup>103</sup>

Although  $\text{TiO}_2$  is a cheap and stable material that can undergo redox reactions, it has a relatively low conductivity, making it a poor target for supercapacitor applications. To this end several modifications have been adopted to benefit from the unique properties of  $\text{TiO}_2$  such as its large surface area.<sup>83-87</sup> Moreover, composites of  $\text{TiO}_2$  nanotube arrays with carbon materials are getting great attention.<sup>106-109</sup>  $\text{TiO}_2$  nanotube arrays usually exhibit a typical rectangular cyclic voltammogram (CV), indicating pseudocapacitive behaviour.<sup>104,110</sup> In addition, it also exhibits minor EDL behaviour which is very beneficial for charge storage.<sup>111</sup> Some studies suggest that intercalation of  $\text{TiO}_2$  with ions in the electrolyte might lead to battery-like behaviour.<sup>112</sup> Meanwhile,  $\text{TiO}_2$  nanotube arrays have low capacitance due to their low conductivity, which motivates researchers to induce modifications to increase their capacitance.<sup>105,110,112-114</sup> Among those modifications is the use of alternative methods to produce titania nanotubes in the powder form.<sup>115</sup> To this end, Wu *et al.*<sup>116</sup> used hydrogen plasma treatment for  $\text{TiO}_2$  nanotubes in order to enhance their capacitive properties. The prepared nanotubes were removed from the surface of Ti foil using adhesive tape then annealed in air at 450 °C. Sequentially, the obtained nanotubes were exposed to a plasma enhanced chemical vapour deposition chamber at 320 °C under vacuum. The hydrogen plasma was then introduced along with hydrogen gas flow. The resulting

hydrogenated  $\text{TiO}_2$  showed a darker colour indicating more defects and it was suggested that the hydrogen atoms were used to passivate the dangling bonds in the shell layer. The phase of the resulting  $\text{TiO}_2$  was mostly anatase, which has higher electrical conductivity. The electrochemical properties of the hydrogenated titania were studied in a three-electrode system in 2 M  $\text{Li}_2\text{SO}_4$  as the electrolyte, Pt foil as the counter electrode, and  $\text{Ag}/\text{AgCl}$  as the reference electrode. The resulting CV showed a quasi-rectangular shape with a potential window of -0.3 to 0.6 V, which indicates high EDL character. The CV curve of the plasma-treated titania was 7.2 times larger than that of the titania powder without treatment. The charge/discharge specific capacitance showed that plasma treatment greatly increased the capacitance of titania nanotubes. The increase in the capacitance was ascribed to the improvement of the conductivity of titania as a result of increasing the number of charge carriers due to the increasing  $\text{Ti}^{3+}$  sites. On the other hand, Dalia El-Gendy *et al.*<sup>117</sup> have used a  $\text{TiO}_2$ /spongy graphene composite for supercapacitor applications. The added graphene enhanced the capacitance of the hydrogenated  $\text{TiO}_2$  powder which reached  $400 \text{ F g}^{-1}$  at a  $1 \text{ mV s}^{-1}$  scan rate and increased the potential window in the positive potential region. The study showed that the  $\text{TiO}_2$  powder affected the behaviour of the cyclic voltammetry curves which deviated from the ideal rectangular shape of ideal EDL electrodes. On the other hand, the study showed that the more the functionalized graphene oxide added to the powdered  $\text{TiO}_2$ , the higher the specific capacitance. Fig. 11 shows the enhancement of the spongy graphene capacitance with the addition of  $\text{TiO}_2$  and the enhancement of the  $\text{TiO}_2$  powder capacitance with increasing the ratio of the functionalized graphene.<sup>117</sup>  $\text{TiO}_2$  powder also showed high performance upon its use in Li-ion batteries. It was shown that allowing  $\text{TiO}_2$  to self-crystallize and relax in its best structure gives the highest diffusion possibility of Li ions into the  $\text{TiO}_2$  crystals. The amorphous cubic structure of  $\text{TiO}_2$  showed

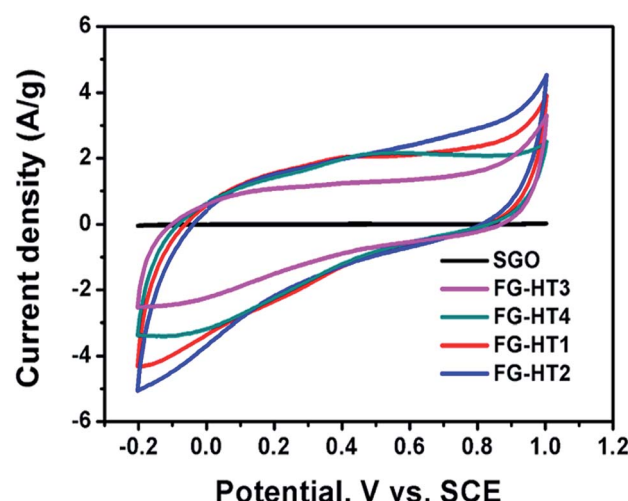


Fig. 11 Cyclic voltammograms of spongy graphene oxide and hydrogenated  $\text{TiO}_2$  with different ratios of functionalized graphene oxide. Reproduced from ref. 117 with permission from the Royal Society of Chemistry.



a specific energy of  $200 \text{ W h kg}^{-1}$  at a specific power of  $30 \text{ W kg}^{-1}$  with high stability over 600 cycles.<sup>118</sup>

## Environmental applications

### Sensing applications

Due to its chemical stability, biocompatibility, and remarkable catalytic properties,<sup>119</sup>  $\text{TiO}_2$  nanotubes have been utilized in different applications, particularly in the powder form.<sup>120</sup> One important example of these applications is sensing platforms, where  $\text{TiO}_2$  nanotubes can be used as a catalyst to bring all the target molecules of the analyte together on their surface to speed up the detection reaction, according to the sensing mechanism, see Fig. 12.<sup>121</sup> In brief, the nanotubular structure of titania, acting as a supporting platform, helps to increase the specific surface area of the sensor and leads to a higher probability of interaction between the target molecules and the TNTP, especially if they are functionalized with another sensitive material.<sup>122</sup> In this case, TNTP will also act as a scaffold to reduce the chances of agglomeration and increase the dispersity of the modifier, as it is usually added in minor amounts. It is worth mentioning that the thin wall thickness of TNTP plays an important role in the sensing mechanism by facilitating the pathways for charge collection after accumulation of the analyte species on the surface.<sup>122</sup> Typically, some ions may attach to the nanotubular nozzles, while some others can be embedded onto the tubular surface. Some ions may even infiltrate inside the tubes to adsorb on the inner tubular walls.<sup>122</sup> All this increases the possibility for the ionic species to be adsorbed and for their charges to be collected on the one-dimensional structure of TNTP. Accordingly, a TNTP-based sensing platform can exhibit high specificity and selectivity toward the species of interest, especially with the enhanced charge collection that the tubular geometry can induce.<sup>29</sup> The sensing strategy itself can be utilized for different purposes. For instance, Abdullah *et al.* have used  $\text{TiO}_2$  nanotube powder in a composite with reduced graphene oxide (RGO) for an environmental approach. The sensing platform was designed against  $\text{Hg}^{(\text{II})}$ ,  $\text{Cu}^{(\text{II})}$ , and  $\text{Mn}^{(\text{II})}$  ions as toxic pollutants in the aquatic environment. The study achieved a limit of detection (LOD) in the ppt level and showed how  $\text{TiO}_2$  nanotubes enhanced the electrocatalytic activity of the

composite *via* acting as a template to minimize the agglomeration of RGO, making use of its low band gap character.<sup>122</sup>  $\text{TiO}_2$  nanotubes have also been employed to enhance the detection of other metals such as  $\text{Fe}^{(\text{III})}$  and  $\text{La}^{(\text{III})}$  by promoting the sensitivity and the ion uptake of the sensors' adsorption sites.<sup>123,124</sup> Additionally, pharmaceutical analyses have utilized  $\text{TiO}_2$  nanotubes in composites to electrochemically determine the concentration of certain drugs such as metformin and benzocaine.<sup>125</sup> The LODs of both studies were as low as  $3 \text{ nM}$  each, which indicates the distinctive electrochemical properties of  $\text{TiO}_2$  nanotubes for such applications. Furthermore,  $\text{TiO}_2$  nanotube powder has been widely used for gas sensing applications. This includes a variety of gases such as hydrogen, acetone, and hydrogen peroxide, either using pristine or metal loaded  $\text{TiO}_2$  nanotube powder.<sup>126</sup> Recently, a study by David *et al.* has proved the enhanced  $\text{H}_2\text{O}_2$  sensing properties of  $\text{TiO}_2$  nanotube powder especially when loaded with Pt. This granted the feasible pathways for electron transfer and enhanced the irreversible nature of the electrochemical reaction.<sup>126</sup> This would pave the way for further functionalization of  $\text{TiO}_2$  nanotube powder using more cost-effective and earth-abundant metals in the near future.

### TNTP for pollutant degradation applications

Due to their unique properties, TNTs have been used extensively in solid phase extraction and degradation of various pollutants in environmental and industrial applications. To be more specific, residual dyes resulting from several industries are perceived as highly undesirable organic pollutants that result in huge quantities of wastewater.<sup>127</sup> For the time being, it is very crucial to turn such wastewater into more useable resources for drinking or irrigation after either degradation or removal of pollutants. For example, Table 2 shows the contribution of reactive dyes to wastewater production due to their low fixation rates in the textile industry.<sup>128</sup>

Nonbiodegradable organic dyes may cause wastewater to have high toxicity to humans, aquatic life and the environment. Their high colour intensity may block sunlight from passing through water which creates restriction for aquatic diversity. It is widely acknowledged that the some of the released aromatic compounds in wastewater are considered toxic, carcinogenic, or mutagenic.<sup>129–131</sup> Hence, the use of such contaminated wastewater may cause different dermal and respiratory diseases in humans.<sup>132</sup> The obstreperous nature of dye wastewater treatment arises from the fact that organic compounds cannot be digested aerobically nor naturally degraded by light.<sup>133</sup> However, photocatalytic degradation of organic dyes by TNTs has been of interest due to their high photon absorption through a large number of active sites.<sup>134–136</sup> In addition, the unique one-dimensional aligned structure helps in increasing photocatalytic efficiency through vertical charge transport resulting in little loss at grain boundaries through recombination.<sup>137–139</sup> The degradation mechanism depends on the electron and hole production upon TNT exposure to light. The produced electrons and holes help reduce  $\text{O}_2$  and oxidize  $\text{H}_2\text{O}$  molecules, respectively. The formed species, typically oxide ions and hydroxyl

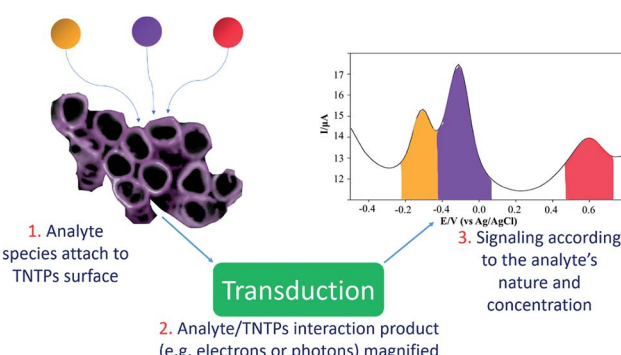


Fig. 12 Schematic representation of the sensing mechanism on TNTP platforms.



Table 2 Mass of dye wastewater from different types of textile dyes

Types of textile dyes	Acid	Reactive	Disperse	Direct	Vat	Basic	Sulfur
Mass of dye water (1000 tons)	20	58	18	20	8	3	40

radicals, have a powerful effect toward organic pollutants, degrading them into their primary molecules such as  $\text{CO}_2$ .<sup>66</sup> A similar mechanism is proposed for the antibacterial effect of TNTP which will be discussed later on. Fig. 13 describes the principal mechanism for using TNTP in the process of environmental disinfection. In 2005, Quan *et al.* explained the higher photo-electrochemical degradation of pentachlorophenol by TNTs in comparison with ordinary  $\text{TiO}_2$  nanoparticles due to their larger kinetics constant.<sup>139</sup> In addition, TNTs have also been proved to exhibit twice the degradation efficiency of  $\text{TiO}_2$  nanoparticles for acid orange dye.<sup>140,141</sup> In order to reduce some of the common limitations of TNTs such as a wide band gap and ability to function effectively only in the UV region, significant efforts have been made to enhance TNTs' photocatalytic activity by anionic/cationic doping or other techniques.<sup>142,143</sup> Different researchers proposed binary systems since they can diminish recombination while accumulating both holes and electrons in two dissimilar layers to enable charge carrier separation.<sup>144–147</sup>

Although introducing impurity levels by cationic dopants might restrict migration of charge carriers if the optimum value is exceeded,<sup>126</sup> it can enhance response in the visible light spectrum. This can be ascribed to the decrease in the lifetime of the electron–hole pairs which was explained through doped sites that may act as recombination sites for charge carriers. Similarly, anion-doped  $\text{TiO}_2$  shows a smaller bandgap than ordinary  $\text{TiO}_2$  which is attributed to the higher potential energy of nanometals that form a new VB closer to the CB. It is believed that anion doping can enhance the photocatalytic activity of TNTs than cationic doping in the visible region, due to the impurity states close to the VB reducing recombination.<sup>127</sup>

Compared to the TNT arrays that are directly attached to the metal substrate, TNTP can exhibit a superior photocatalytic performance in the degradation of organic pollutants. This

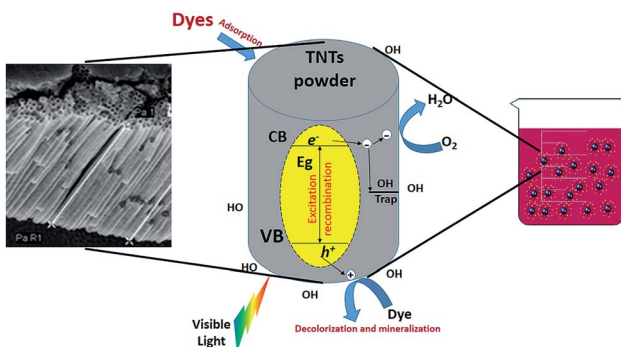


Fig. 13 The principal mechanism for using TNTP in the process of environmental disinfection.

enhancement was ascribed to the higher surface area of the latter. As annealing at high temperatures of the TNT arrays attached to the Ti metal substrate leads to crystallite growth in the TNT walls resulting in increased tube wall thickness and subsequently decreased surface area.<sup>14</sup> Another drawback that can lower the photocatalytic activity of TNT arrays attached to the Ti substrate is that the transformation from the anatase phase to the rutile one upon annealing above 550 °C.<sup>147–149</sup> Destabilizing the anatase phase of the TNTs results in shrinking of their photocatalytic activity.<sup>150,151</sup>

Jia *et al.*<sup>14</sup> studied the effect of annealing temperature on the crystal structure and the photocatalytic performance of the TNTP. The TNTs were prepared *via* the anodization technique followed by sonication in ethanol in order to remove the nanotube layer and then the as-prepared TNTP were subjected to different annealing temperatures (450, 550, 650 and 750 °C) for 2 h in air.

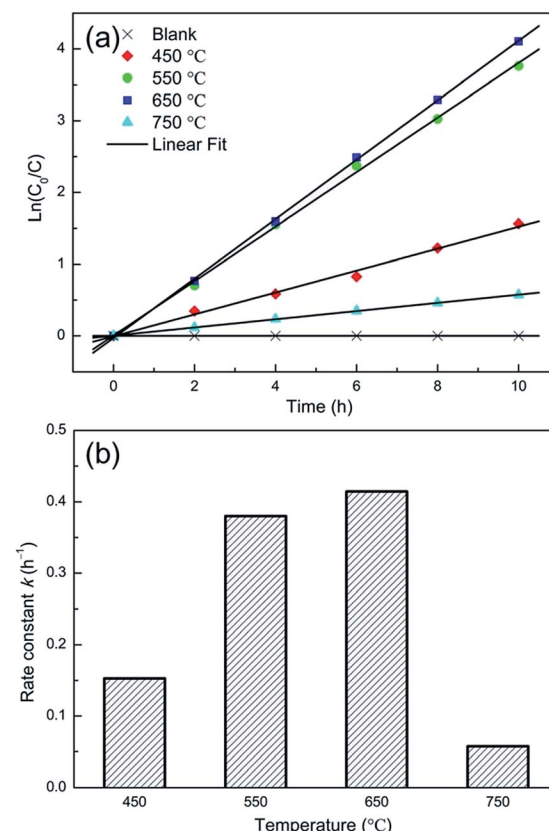


Fig. 14 (a) Time dependent MB concentration showing the photocatalytic decomposition kinetic behaviour of the NT powders obtained at various annealing temperatures; (b) the photocatalytic rate constant. Reproduced from ref. 14 with permission from the Springer Publishing group under Creative Commons Attribution 4.0 International License.



The SEM and XRD patterns showed that all the samples conserved the tubular morphology and the anatase crystal structure upon annealing up to 750 °C, respectively. Despite the decreased specific surface area of the TNTs upon increasing the annealing temperature up to 750 °C, the samples showed enhanced photocatalytic degradation of methylene blue upon increasing the annealing temperature up to 650 °C. This indicates the superior effect of the enhanced crystallinity compared to the effect of the specific surface area as shown in Fig. 14.<sup>14</sup>

Liang *et al.*<sup>93</sup> demonstrated the effect of doping TNTP with cobalt ions on the photocatalytic degradation of methylene blue under UV irradiation. The co-precipitation method followed by hydrothermal treatment was used to fabricate un-doped and Co-doped TNTP. The as-prepared samples were annealed at 450 °C for 3 h. The XRD patterns were indexed to the anatase phase and confirmed that doping with cobalt ions at low concentrations does not affect the crystal structure of the TNTs. Doping TNTs with Co ions at concentrations up to 1.3% increased the photocatalytic degradation rate of methylene blue up to 97.2% compared to the un-doped TNTs' 80.6% under UV irradiation.<sup>93</sup>

## Conclusions & future perspectives

TNTP are a type of semiconducting material that can offer advantages such as feasible synthesis, low cost, and promising performance for a variety of applications. This review recapitulates the cutting-edge knowledge about TNTP developed and experimentally tested. Fabrication methods such as ultrasonication, hydrothermal processing, and rapid breakdown anodization have been summarized and the properties of the produced TNTP were further discussed. Effects of synthesis techniques and defect structures on TNTP for biological applications were reviewed. More investigation is needed to evaluate how TNTP can be better utilized as drug carriers and sensing substrates where TiO<sub>2</sub> is currently a predominant platform. Based on the biological advantages of TNTP, using them for antibacterial approaches has been discussed. The review also demonstrated the auspicious performance of TNTP for energy conversion applications. This is expected to be more effective upon better fundamental understanding and control of TNTP structural parameters such as anchoring, sensitization, decoration and functionalization. The effect of TNTP preparation conditions on their capacitance and organic degradation applications has also been overviewed. Comparative studies between TNTP and TNT arrays would be useful to assess the former's efficiency when produced with other fabrication techniques and under other treatment conditions such as annealing parameters, defect formation, and phase change. One of the important future insights is to synthesize mixed oxide nanotube powder to enhance the optical, electrical, and electrochemical performance of TiO<sub>2</sub> nanotubes. Another future trend could be the development of various protocols to dope the TiO<sub>2</sub> nanotube powder with foreign elements for various applications.

## Conflicts of interest

The authors declare no conflict of interest.

## References

- 1 T. Wang, *et al.*, Controlled release and biocompatibility of polymer/titania nanotube array system on titanium implants, *Bioact. Mater.*, 2017, **2**, 44–50.
- 2 C. Yao and T. J. Webster, Anodization: A Promising Nano-Modification Technique of Titanium Implants for Orthopedic Applications, *J. Nanosci. Nanotechnol.*, 2006, **6**, 2682–2692.
- 3 D. Losic and S. Simovic, Self-ordered nanopore and nanotube platforms for drug delivery applications, *Expert Opin. Drug Delivery*, 2009, **6**, 1363–1381.
- 4 C. López de Dicastillo, *et al.*, Novel Antimicrobial Titanium Dioxide Nanotubes Obtained through a Combination of Atomic Layer Deposition and Electrospinning Technologies, *Nanomaterials*, 2018, **8**, 128.
- 5 A. A. Al-Swaih, Electrochemical behavior of self-ordered titania nanotubes prepared by anodization as a promising material for biomedical applications, *J. Am. Sci.*, 2014, **10**, 165–173.
- 6 P. Xiao, B. B. Garcia, Q. Guo, D. Liu and G. Cao, TiO<sub>2</sub> nanotube arrays fabricated by anodization in different electrolytes for biosensing, *Electrochem. Commun.*, 2007, **9**, 2441–2447.
- 7 P. Xiao, Y. Zhang and G. Cao, Effect of surface defects on biosensing properties of TiO<sub>2</sub> nanotube arrays, *Sens. Actuators, B*, 2011, **155**, 159–164.
- 8 S. Sreekantan, K. A. Saharudin and L. C. Wei, Formation of TiO<sub>2</sub> nanotubes via anodization and potential applications for photocatalysts, biomedical materials, and photoelectrochemical cell, *IOP Conf. Ser.: Mater. Sci. Eng.*, 2011, **21**, 012002.
- 9 C. Lin and W. Lin, Sun Protection Factor Analysis of Sunscreens Containing Titanium Dioxide Nanoparticles, *J. Food Drug Anal.*, 2011, **19**, 1–8.
- 10 Y. Lin, J. Ma, W. Liu, Z. Li and K. He, Efficient removal of dyes from dyeing wastewater by powder activated charcoal/titanate nanotube nanocomposites: adsorption and photoregeneration, *Environ. Sci. Pollut. Res.*, 2019, **26**, 10263–10273.
- 11 H. L. Hoşgün and M. T. A. Aydin, Synthesis, characterization and photocatalytic activity of boron-doped titanium dioxide nanotubes, *J. Mol. Struct.*, 2019, **1180**, 676–682.
- 12 K. Fischer, *et al.*, Low-Temperature Synthesis of Anatase/Rutile/Brookite TiO<sub>2</sub> Nanoparticles on a Polymer Membrane for Photocatalysis, *Catalysts*, 2017, **7**, 209.
- 13 U. M. Garusinghe, V. S. Raghuvanshi, W. Batchelor and G. Garnier, Water Resistant Cellulose–Titanium Dioxide Composites for Photocatalysis, *Sci. Rep.*, 2018, **8**, 1–13.
- 14 J. Lin, X. Liu, S. Zhu, Y. Liu and X. Chen, Anatase TiO<sub>2</sub> nanotube powder film with high crystallinity for enhanced photocatalytic performance, *Nanoscale Res. Lett.*, 2015, **10**, 110.
- 15 N. F. Fahim and T. Sekino, A Novel Method for Synthesis of Titania Nanotube Powders using Rapid Breakdown Anodization, *Chem. Mater.*, 2009, **21**, 1967–1979.



16 R. P. Antony, *et al.*, Rapid breakdown anodization technique for the synthesis of high aspect ratio and high surface area anatase  $\text{TiO}_2$  nanotube powders, *J. Solid State Chem.*, 2011, **184**, 624–632.

17 K. C. Sun, M. B. Qadir and S. H. Jeong, Hydrothermal synthesis of  $\text{TiO}_2$  nanotubes and their application as an over-layer for dye-sensitized solar cells, *RSC Adv.*, 2014, **4**, 23223.

18 J. Yang, *et al.*, Highly Hydrophilic  $\text{TiO}_2$  Nanotubes Network by Alkaline Hydrothermal Method for Photocatalysis Degradation of Methyl Orange, *Nanomaterials*, 2019, **9**, 526.

19 S. Wu, Z. Weng, X. Liu, K. W. K. Yeung and P. K. Chu, Functionalized  $\text{TiO}_2$  Based Nanomaterials for Biomedical Applications, *Adv. Funct. Mater.*, 2014, **24**, 5464–5481.

20 S. I. Matsushita, T. Miwa, D. A. Tryk and A. Fujishima, New mesostructured porous  $\text{TiO}_2$  surface prepared using a two-dimensional array-based template of silica particles, *Langmuir*, 1998, **14**, 6441–6447.

21 H. Hayashi and K. Torii, Hydrothermal synthesis of titania photocatalyst under subcritical and supercritical water conditions, *J. Mater. Chem.*, 2002, **12**, 3671–3676.

22 W. Light, *Hydrogen*, Springer, US, 2008, DOI: 10.1007/978-0-387-68238-9.

23 T. J. Webster and C. A. Yao, A promising nano modification technique of titanium-based implants for orthopedic applications, in *Surgical Tools and Medical Devices*, 2nd edn, 2016, vol. 6, pp. 55–80.

24 N. K. Allam and C. A. Grimes, Formation of Vertically Oriented  $\text{TiO}_2$  Nanotube Arrays using a Fluoride Free HCl Aqueous Electrolyte, *J. Phys. Chem. C*, 2007, **111**, 13028–13032.

25 S. Minagar, C. C. Berndt, J. Wang, E. Ivanova and C. Wen, A review of the application of anodization for the fabrication of nanotubes on metal implant surfaces, *Acta Biomater.*, 2012, **8**, 2875–2888.

26 L. Yang, S. Luo, Q. Cai and S. Yao, A review on  $\text{TiO}_2$  nanotube arrays: Fabrication, properties, and sensing applications, *Chin. Sci. Bull.*, 2010, **55**, 331–338.

27 H. E. Prakasam, K. Shankar, M. Paulose, O. K. Varghese and C. A. Grimes, A New Benchmark for  $\text{TiO}_2$  Nanotube Array Growth by Anodization, *J. Phys. Chem. C*, 2007, **111**, 7235–7241.

28 M. Samir, M. Salama and N. K. Allam, Sub-100 nm  $\text{TiO}_2$  tubular architectures for efficient solar energy conversion, *J. Mater. Chem. A*, 2016, **4**, 9375–9380.

29 A. M. Mohamed, A. S. Aljaber, S. Y. Alqaradawi and N. K. Allam,  $\text{TiO}_2$  Nanotubes with Ultrathin Walls for Enhanced Water Splitting, *Chem. Commun.*, 2015, **51**, 12617–12620.

30 D. Gong, *et al.*, Titanium oxide nanotube arrays prepared by anodic oxidation, *J. Mater. Res.*, 2001, **16**, 3331–3334.

31 Q. Cai, M. Paulose, O. K. Varghese and C. A. Grimes, The effect of electrolyte composition on the fabrication of self-organized titanium oxide nanotube arrays by anodic oxidation, *J. Mater. Res.*, 2005, **20**, 230–236.

32 D. Pathinettam Padiyan and D. Henry Raja, Synthesis of various generations titania nanotube arrays by electrochemical anodization for  $\text{H}_2$  production, *Energy Procedia*, 2011, **22**, 88–100.

33 J. Wang and Z. Lin, Freestanding  $\text{TiO}_2$  Nanotube Arrays with Ultrahigh Aspect Ratio via Electrochemical Anodization, *Chem. Mater.*, 2008, **20**, 1257–1261.

34 J. M. Macak, M. Zlamal, J. Krysa and P. Schmuki, Self-organized  $\text{TiO}_2$  nanotube layers as highly efficient photocatalysts, *Small*, 2007, **3**, 300–304.

35 J. M. Macák, H. Tsuchiya and P. Schmuki, High-aspect-ratio  $\text{TiO}_2$  nanotubes by anodization of titanium, *Angew. Chem., Int. Ed.*, 2005, **44**, 2100–2102.

36 M. Paulose, *et al.*,  $\text{TiO}_2$  nanotube arrays of 1000  $\mu\text{m}$  length by anodization of titanium foil: Phenol red diffusion, *J. Phys. Chem. C*, 2007, **111**, 14992–14997.

37 J. M. Macák and P. Schmuki, Anodic growth of self-organized anodic  $\text{TiO}_2$  nanotubes in viscous electrolytes, *Electrochim. Acta*, 2006, **52**, 1258–1264.

38 N. F. Fahim, T. Sekino, M. F. Morks and T. Kusunose, Electrochemical Growth of Vertically-Oriented High Aspect Ratio Titania Nanotubes by Rabid Anodization in Fluoride-Free Media, *J. Nanosci. Nanotechnol.*, 2009, **9**, 1803–1818.

39 M. Á. López Zavala, S. A. Lozano Morales and M. Ávila-Santos, Synthesis of stable  $\text{TiO}_2$  nanotubes: effect of hydrothermal treatment, acid washing and annealing temperature, *Helijon*, 2017, **3**, e00456.

40 Y. Q. Wang, G. Q. Hu, X. F. Duan, H. L. Sun and Q. K. Xue, Microstructure and formation mechanism of titanium dioxide nanotubes, *Chem. Phys. Lett.*, 2002, **365**, 427–431.

41 T. Kasuga, M. Hiramatsu, A. Hoson, T. Sekino and K. Niihara, Formation of Titanium Oxide Nanotube, *Langmuir*, 1998, **14**, 3160–3163.

42 M. Moazeni, H. Hajipour, M. Askari and M. Nusheh, Hydrothermal synthesis and characterization of titanium dioxide nanotubes as novel lithium adsorbents, *Mater. Res. Bull.*, 2015, **61**, 70–75.

43 Y.-Z. Zeng, Y.-C. Liu, Y.-F. Lu and J.-C. Chung, Study on the Preparation of Nanosized Titanium Dioxide with Tubular Structure by Hydrothermal Method and Their Photocatalytic Activity, *Int. J. Chem. Eng. Appl.*, 2014, **5**, 234–239.

44 N. Viriya-empikul, *et al.*, Effect of preparation variables on morphology and anatase–brookite phase transition in sonication assisted hydrothermal reaction for synthesis of titanate nanostructures, *Mater. Chem. Phys.*, 2009, **118**, 254–258.

45 L. Torrente-Murciano, A. A. Lapkin and D. Chadwick, Synthesis of high aspect ratio titanate nanotubes, *J. Mater. Chem.*, 2010, **20**, 6484–6489.

46 Y. Tang, *et al.*, Unravelling the correlation between the aspect ratio of nanotubular structures and their electrochemical performance to achieve high-rate and long-life lithium-ion batteries, *Angew. Chem., Int. Ed.*, 2014, **53**, 13488–13492.

47 D. Losic, M. S. Aw, A. Santos, K. Gulati and M. Bariana, Titania nanotube arrays for local drug delivery: recent



advances and perspectives, *Expert Opin. Drug Delivery*, 2015, **12**, 103–127.

48 H. Jia and L. L. Kerr, Sustained ibuprofen release using composite poly(lactic-co-glycolic acid)/titanium dioxide nanotubes from Ti implant surface, *J. Pharm. Sci.*, 2013, **102**, 2341–2348.

49 C. Moseke, F. Hage, E. Vorndran and U. Gbureck, TiO<sub>2</sub> nanotube arrays deposited on Ti substrate by anodic oxidation and their potential as a long-term drug delivery system for antimicrobial agents, *Appl. Surf. Sci.*, 2012, **258**, 5399–5404.

50 A. Hamlekhan, *et al.*, Fabrication of drug eluting implants: Study of drug release mechanism from titanium dioxide nanotubes, *J. Phys. D: Appl. Phys.*, 2015, **48**, 275401.

51 N. Çalışkan, C. Bayram, E. Erdal, Z. Karahaliloglu and E. B. Denkbaş, Titania nanotubes with adjustable dimensions for drug reservoir sites and enhanced cell adhesion, *Mater. Sci. Eng., C*, 2014, **35**, 100–105.

52 A. M. Sinn, M. Kurian and D. Losic, Non-eroding drug-releasing implants with ordered nanoporous and nanotubular structures: Concepts for controlling drug release, *Biomater. Sci.*, 2014, **2**, 10–34.

53 E. Ajami and K. F. Aguey-Zinsou, Functionalization of electropolished titanium surfaces with silane-based self-assembled monolayers and their application in drug delivery, *J. Colloid Interface Sci.*, 2012, **385**, 258–267.

54 M. Gary-Bobo, *et al.*, Cancer therapy improvement with mesoporous silica nanoparticles combining targeting, drug delivery and PDT, *Int. J. Pharm.*, 2012, **423**, 509–515.

55 P. W. Kämmerer, *et al.*, Early implant healing: Promotion of platelet activation and cytokine release by topographical, chemical and biomimetical titanium surface modifications in vitro, *Clin. Oral Implants Res.*, 2012, **23**, 504–510.

56 S. Sirivisoot, R. Parea and T. Webster, Electrically controlled drug release from nanostructured polypyrrole coated on titanium, *Nanotechnology*, 2011, **22**, 85–101.

57 M. S. Aw and D. Losic, Ultrasound enhanced release of therapeutics from drug-releasing implants based on titania nanotube arrays, *Int. J. Pharm.*, 2013, **443**, 154–162.

58 X. Li, L. Wang, Y. Fan, Q. Feng and F. Z. Cui, Biocompatibility and toxicity of nanoparticles and nanotubes, *J. Nanomater.*, 2012, **2012**, 548389.

59 E. Feschet-Chassot, *et al.*, Tunable functionality and toxicity studies of titanium dioxide nanotube layers, *Thin Solid Films*, 2011, **519**, 2564–2568.

60 W. Chen, X. Yu, Z. Zhao, S. Ji and L. Feng, Hierarchical architecture of coupling graphene and 2D WS<sub>2</sub> for high-performance supercapacitor, *Electrochim. Acta*, 2019, **298**, 313–320.

61 N. Thi-Tuyet Hoang, A. Thi-Kim Tran, N. Van Suc and T.-V. Nguyen, Antibacterial activities of gel-derived Ag-TiO<sub>2</sub>-SiO<sub>2</sub> nanomaterials under different light irradiation, *AIMS Mater. Sci.*, 2016, **3**, 339–348.

62 S. Bonetta, S. Bonetta, F. Motta, A. Strini and E. Carraro, Photocatalytic bacterial inactivation by TiO<sub>2</sub>-coated surfaces, *AMB Express*, 2013, **3**, 1–8.

63 W. S. Lee, Y.-S. Park and Y.-K. Cho, Significantly enhanced antibacterial activity of TiO<sub>2</sub> nanofibers with hierarchical nanostructures and controlled crystallinity, *Analyst*, 2015, **140**, 616–622.

64 J. W. Liou and H. H. Chang, Bactericidal effects and mechanisms of visible light-responsive titanium dioxide photocatalysts on pathogenic bacteria, *Arch. Immunol. Ther. Exp.*, 2012, **60**, 267–275.

65 D. Yañez, *et al.*, Photocatalytic inhibition of bacteria by TiO<sub>2</sub> nanotubes-doped polyethylene composites, *Appl. Catal., A*, 2015, **489**, 255–261.

66 M. N. Chong, B. Jin, C. W. K. Chow and C. Saint, Recent developments in photocatalytic water treatment technology: A review, *Water Res.*, 2010, **44**, 2997–3027.

67 W. Deng, *et al.*, I-TiO<sub>2</sub>/PVC film with highly photocatalytic antibacterial activity under visible light, *Colloids Surf., B*, 2016, **144**, 196–202.

68 C. Zhao, *et al.*, Preparation and antibacterial activity of titanium nanotubes loaded with Ag nanoparticles in the dark and under the UV light, *Appl. Surf. Sci.*, 2013, **280**, 8–14.

69 J. Podporska-Carroll, *et al.*, Antimicrobial properties of highly efficient photocatalytic TiO<sub>2</sub> nanotubes, *Appl. Catal., B*, 2015, **176–177**, 70–75.

70 W. A. Abbas, *et al.*, Photoactive catalysts for effective water microbial purification: Morphology-activity relationship, *Environmental Nanotechnology, Monitoring and Management*, 2018, **10**, 87–93.

71 J. Desilvestro, M. Grätzel, L. Kavan, J. Moser and J. Augustynski, Highly Efficient Sensitization of Titanium Dioxide, *J. Am. Chem. Soc.*, 1985, **107**, 2988–2990.

72 B. O'Regan and M. Grätzel, A low-cost, high-efficiency solar cell based on dye-sensitized colloidal TiO<sub>2</sub> films, *Nature*, 1991, **353**, 737–740.

73 Y. Chiba, *et al.*, Dye-sensitized solar cells with conversion efficiency of 11.1%, *Jpn. J. Appl. Phys., Part 2*, 2006, **45**, L638–L640.

74 M. Grätzel, Solar energy conversion by dye-sensitized photovoltaic cells, *Inorg. Chem.*, 2005, **44**, 6841–6851.

75 A. Vonarbourg, C. Passirani, P. Saulnier and J. P. Benoit, Parameters influencing the stealthiness of colloidal drug delivery systems, *Biomaterials*, 2006, **27**, 4356–4373.

76 J. Bisquert, Fractional Diffusion in the Multiple-Trapping Regime and Revision of the Equivalence with the Continuous-Time Random Walk, *Phys. Rev. Lett.*, 2003, **91**, 010602.

77 J. Nelson, Continuous-time random-walk model of electron transport in nanocrystalline TiO<sub>2</sub> electrodes, *Phys. Rev. B: Condens. Matter Mater. Phys.*, 1999, **59**, 15374–15380.

78 A. Ghicov and P. Schmuki, Self-ordering electrochemistry: a review on growth and functionality of TiO<sub>2</sub> nanotubes and other self-aligned MO<sub>x</sub> structures, *Chem. Commun.*, 2009, 2791, DOI: 10.1039/b822726h.

79 N. K. Awad, E. A. Ashour and K. Allam, Recent Advances in the Use of Metal Oxide-Based Photocathodes for Solar Fuel Production, *J. Renewable Sustainable Energy*, 2014, **6**, 022702.



80 R. Hahn, *et al.*, Efficient solar energy conversion using  $TiO_2$  nanotubes produced by rapid breakdown anodization – A comparison, *Phys. Status Solidi RRL*, 2007, **1**, 135–137.

81 W. J. Lee, E. Ramasamy and D. Y. Lee, Effect of electrode geometry on the photovoltaic performance of dye-sensitized solar cells, *Sol. Energy Mater. Sol. Cells*, 2009, **93**, 1448–1451.

82 C. Z. Zhao, *et al.*, Dielectric relaxation of La-doped zirconia caused by annealing ambient, *Nanoscale Res. Lett.*, 2012, **7**, 1–6.

83 J. Hu, *et al.*,  $TiO_2$  nanotube/ $TiO_2$  nanoparticle hybrid photoanode for hole-conductor-free perovskite solar cells based on carbon counter electrodes, *Opt. Mater. Express*, 2017, **7**, 3322.

84 S. Kumar, T. Vats, S. N. Sharma and J. Kumar, Investigation of annealing effects on  $TiO_2$  nanotubes synthesized by a hydrothermal method for hybrid solar cells, *Optik*, 2018, **171**, 492–500.

85 M. F. Goes, M. A. Sinhoreti, S. Consani and M. A. Silva, Morphological effect of the type, concentration and etching time of acid solutions on enamel and dentin surfaces, *Braz. Dent. J.*, 1998, **9**, 3–10.

86 K. C. Christoforidis and P. Fornasiero, Photocatalytic Hydrogen Production: A Rift into the Future Energy Supply, *ChemCatChem*, 2017, **9**, 1523–1544.

87 K. Maeda and K. Domen, New non-oxide photocatalysts designed for overall water splitting under visible light, *J. Phys. Chem. C*, 2007, **111**, 7851–7861.

88 C. A. Grimes, O. K. Varghese and S. Ranjan, *Light, water, hydrogen: The solar generation of hydrogen by water photoelectrolysis*, 2008, DOI: 10.1007/978-0-387-68238-9.

89 H. A. Hamedani, *et al.*, An Experimental Insight into the Structural and Electronic Characteristics of Strontium-Doped Titanium Dioxide Nanotube Arrays, *Adv. Funct. Mater.*, 2014, **24**, 6783–6796.

90 C. M. Teh and A. R. Mohamed, Roles of titanium dioxide and ion-doped titanium dioxide on photocatalytic degradation of organic pollutants (phenolic compounds and dyes) in aqueous solutions: A review, *J. Alloys Compd.*, 2011, **509**, 1648–1660.

91 J. Tian, *et al.*, Ru nanoparticles decorated  $TiO_2$  nanobelts: A heterostructure towards enhanced photocatalytic activity and gas-phase selective oxidation of benzyl alcohol, *Ceram. Int.*, 2016, **42**, 1611–1617.

92 S. Cho, J. W. Jang, K. H. Lee and J. S. Lee, Research update: Strategies for efficient photoelectrochemical water splitting using metal oxide photoanodes, *APL Mater.*, 2014, **2**, 010703.

93 J. Liang, C. Hao, K. Yu and Y. Li, Excellent photocatalytic performance of cobalt-doped titanium dioxide nanotubes under ultraviolet light, *Nanomater. Nanotechnol.*, 2016, **6**, 1847980416680808.

94 L. K. Preethi, R. P. Antony, T. Mathews, L. Walczak and C. S. Gopinath, A Study on Doped Heterojunctions in  $TiO_2$  Nanotubes: An Efficient Photocatalyst for Solar Water Splitting, *Sci. Rep.*, 2017, **7**, 14314.

95 T. M. David, *et al.*, Photocatalytic water splitting of  $TiO_2$  nanotubes powders prepared via rapid breakdown anodization sensitized with Pt, Pd and Ni nanoparticles, *Mater. Technol.*, 2018, **7857**, 1–13.

96 Y. Wang, Y. Song and Y. Xia, Electrochemical capacitors: mechanism, materials, systems, characterization and applications, *Chem. Soc. Rev.*, 2016, **45**, 5925–5950.

97 C. G. Cameron, Electrochemical Capacitors, in *Springer Handbook of Electrochemical Energy*, Springer, Berlin, Heidelberg, 2017, pp. 563–589, DOI: 10.1007/978-3-662-46657-5\_17.

98 S. Zhang and N. Pan, Supercapacitors performance evaluation, *Adv. Energy Mater.*, 2015, **5**, 1–19.

99 E. Goikolea and R. Mysyk, Chapter Four – Nanotechnology in Electrochemical Capacitors A2 – Rodriguez-Martinez, Lide M, in *Micro and Nano Technologies*, ed. L. M. Rodriguez-Martinez and N. Omar, Elsevier, 2017, pp. 131–169, DOI: 10.1016/B978-0-323-42977-1.00004-2.

100 N. Ahmed, B. A. Ali, M. Ramadan and N. K. Allam, Three-Dimensional Interconnected Binder-Free Mn–Ni–S Nanosheets for High-Performance Asymmetric Supercapacitors with Exceptional Cyclic Stability, *ACS Appl. Energy Mater.*, 2019, **25**, 3717–3725.

101 B. A. Ali, O. I. Metwalli, A. S. G. Khalil and N. K. Allam, Unveiling the Effect of the Structure of Carbon Material on the Charge Storage Mechanism in  $MoS_2$ -Based Supercapacitors, *ACS Omega*, 2018, **3**, 16301–16308.

102 T. Brousse, D. Belanger and J. W. Long, To Be or Not To Be Pseudocapacitive?, *J. Electrochem. Soc.*, 2015, **162**, A5185–A5189.

103 S. Liu, S. Sun and X.-Z. You, Inorganic nanostructured materials for high performance electrochemical supercapacitors, *Nanoscale*, 2014, **6**, 2037.

104 Z. Li, *et al.*, Reduction Mechanism and Capacitive Properties of Highly Electrochemically Reduced  $TiO_2$  Nanotube Arrays, *Electrochim. Acta*, 2015, **161**, 40–47.

105 M. Z. Ge, *et al.*, Synthesis, modification, and photo/photoelectrocatalytic degradation applications of  $TiO_2$  nanotube arrays: A review, *Nanotechnol. Rev.*, 2016, **5**, 75–112.

106 A. Ramadoss and S. J. Kim, Vertically aligned  $TiO_2$  nanorod arrays for electrochemical supercapacitor, *J. Alloys Compd.*, 2013, **561**, 262–267.

107 M. Zhou, A. M. Glushenkov, O. Kartachova, Y. Li and Y. Chen, Titanium Dioxide Nanotube Films for Electrochemical Supercapacitors: Biocompatibility and Operation in an Electrolyte Based on a Physiological Fluid, *J. Electrochem. Soc.*, 2015, **162**, A5065–A5069.

108 B. Gao, *et al.*,  $MnO_2$ – $TiO_2$ /C nanocomposite arrays for high-performance supercapacitor electrodes, *Thin Solid Films*, 2015, **584**, 61–65.

109 H. Xiao, W. Guo, B. Sun, M. Pei and G. Zhou, Mesoporous  $TiO_2$  and Co-doped  $TiO_2$  Nanotubes/Reduced Graphene Oxide Composites as Electrodes for Supercapacitors, *Electrochim. Acta*, 2016, **190**, 104–117.



110 H. Zhou and Y. Zhang, Enhancing the capacitance of  $\text{TiO}_2$  nanotube arrays by a facile cathodic reduction process, *J. Power Sources*, 2013, **239**, 128–131.

111 B. E. Conway and W. G. Pell, Double-layer and pseudocapacitance types of electrochemical capacitors and their applications to the development of hybrid devices, *J. Solid State Electrochem.*, 2003, **7**, 637–644.

112 T. Brezesinski, J. Wang, S. H. Tolbert and B. Dunn, Next generation pseudocapacitor materials from sol-gel derived transition metal oxides, *J. Sol-Gel Sci. Technol.*, 2011, **57**, 330–335.

113 M. Salari, S. H. Aboutalebi, A. T. Chidembo, K. Konstantinov and H. K. Liu, Surface engineering of self-assembled  $\text{TiO}_2$  nanotube arrays: A practical route towards energy storage applications, *J. Alloys Compd.*, 2014, **586**, 197–201.

114 X. Lu, *et al.*, Hydrogenated  $\text{TiO}_2$  Nanotube Arrays for Supercapacitors, *Nano Lett.*, 2012, **12**, 1690–1696.

115 M. Salari, S. H. Aboutalebi, K. Konstantinov and H. K. Liu, A highly ordered titania nanotube array as a supercapacitor electrode, *Phys. Chem. Chem. Phys.*, 2011, **13**, 5038.

116 H. Wu, *et al.*, Enhanced supercapacitance in anodic  $\text{TiO}_2$  nanotube films by hydrogen plasma treatment, *Nanotechnology*, 2013, **24**, 455401.

117 D. M. El-Gendy, N. A. A. Ghany and N. K. Allam, Black titania nanotubes/spongy graphene nanocomposites for high-performance supercapacitors, *RSC Adv.*, 2019, **9**, 12555–12566.

118 H. Xiong, *et al.*, Self-Improving Anode for Lithium-Ion Batteries Based on Amorphous to Cubic Phase Transition in  $\text{TiO}_2$  Nanotubes, *J. Phys. Chem. C*, 2012, **116**, 3181–3187.

119 M. A. Mohamed, *et al.*, Smart bi-metallic perovskite nanofibers as selective and reusable sensors of nano-level concentrations of non-steroidal anti-inflammatory drugs, *Talanta*, 2018, **185**, 344–351.

120 P. Zhong, Y. Liao, W. Que, Q. Jia and T. Lei, Enhanced electron collection in photoanode based on ultrafine  $\text{TiO}_2$  nanotubes by a rapid anodization process, *J. Solid State Electrochem.*, 2014, **18**, 2087–2098.

121 N. Liu, X. Chen, J. Zhang and J. W. Schwank, A review on  $\text{TiO}_2$ -based nanotubes synthesized via hydrothermal method: Formation mechanism, structure modification, and photocatalytic applications, *Catal. Today*, 2014, **225**, 34–51.

122 I. Abdullah, *et al.*, Engineered Nanocomposite for Sensitive and Selective Detection of Mercury in Environmental Water Samples, *Anal. Methods*, 2018, **10**, 2526–2535.

123 M. M. Rahman, S. B. Khan, H. M. Marwani, A. M. Asiri and K. A. Alamry, Selective Iron(III) ion uptake using  $\text{CuO}-\text{TiO}_2$  nanostructure by inductively coupled plasma-optical emission spectrometry, *Chem. Cent. J.*, 2012, **6**, 158.

124 M. M. Rahman,  $\text{SnO}_2-\text{TiO}_2$  nanocomposites as new adsorbent for efficient removal of La(III) ions from aqueous solutions, *J. Taiwan Inst. Chem. Eng.*, 2014, **45**, 1964–1974.

125 M. Shamsipur, M. B. Gholivand, S. Dehdashtian, M. Feyzi and F. Jafari, Synthesis of Co/TiO<sub>2</sub> Nanocomposite and its Use in Construction of a Sensitive and Selective Sensor for Determination of Ciprofloxacin, *Adv. Mater. Res.*, 2013, **829**, 563–567.

126 T. M. David, *et al.*, Electrocatalytic Investigation of Group X Metal Nanoparticles Loaded  $\text{TiO}_2$  Nanotubes Powder Prepared by Rapid Breakdown Anodization for Selective  $\text{H}_2\text{O}_2$  Sensing, *J. Electrochem. Soc.*, 2017, **164**, B356–B365.

127 Z. Carmen and S. Daniel, Textile Organic Dyes – Characteristics, Polluting Effects and Separation/Elimination Procedures from Industrial Effluents – A Critical Overview, in *Organic Pollutants Ten Years after the Stockholm Convention – Environmental and Analytical Update*, InTech, 2012, DOI: 10.5772/32373.

128 S. Vanhulle, *et al.*, Decolorization, cytotoxicity, and genotoxicity reduction during a combined ozonation/fungal treatment of dye-contaminated wastewater, *Environ. Sci. Technol.*, 2008, **42**, 584–589.

129 B. Manu and S. Chaudhari, Anaerobic decolorisation of simulated textile wastewater containing azo dyes, *Bioresour. Technol.*, 2002, **82**, 225–231.

130 D. Suteu, C. Zaharia and T. Malutan, Removal of Orange 16 reactive dye from aqueous solutions by waste sunflower seed shells, *J. Serb. Chem. Soc.*, 2011, **76**, 607–624.

131 A. Asghar, A. A. A. Raman and W. M. A. W. Daud, Advanced oxidation processes for in-situ production of hydrogen peroxide/hydroxyl radical for textile wastewater treatment: A review, *J. Cleaner Prod.*, 2015, **87**, 826–838.

132 S. Merouani, O. Hamdaoui, F. Saoudi, M. Chiha and C. Pétrier, Influence of bicarbonate and carbonate ions on sonochemical degradation of Rhodamine B in aqueous phase, *J. Hazard. Mater.*, 2010, **175**, 593–599.

133 S. M. Ghoreishi and R. Haghghi, Chemical catalytic reaction and biological oxidation for treatment of non-biodegradable textile effluent, *Chem. Eng. J.*, 2003, **95**, 163–169.

134 L. Sun, S. Zhang, X. Sun and X. He, Effect of the Geometry of the Anodized Titania Nanotube Array on the Performance of Dye-Sensitized Solar Cells, *J. Nanosci. Nanotechnol.*, 2010, **10**, 4551–4561.

135 A. Nakahira, T. Kubo and C. Numako, Formation mechanism of  $\text{TiO}_2$ -derived titanate nanotubes prepared by the hydrothermal process, *Inorg. Chem.*, 2010, **49**, 5845–5852.

136 S. So, K. Lee and P. Schmuki, Ultrafast growth of highly ordered anodic  $\text{TiO}_2$  nanotubes in lactic acid electrolytes, *J. Am. Chem. Soc.*, 2012, **134**, 11316–11318.

137 A. El Ruby Mohamed and S. Rohani, Modified  $\text{TiO}_2$  nanotube arrays (TNTAs): Progressive strategies towards visible light responsive photoanode, a review, *Energy Environ. Sci.*, 2011, **4**, 1065–1086.

138 P. Roy, S. Berger and P. Schmuki,  $\text{TiO}_2$  nanotubes: Synthesis and applications, *Angew. Chem., Int. Ed.*, 2011, **50**, 2904–2939.

139 X. Quan, S. Yang, X. Ruan and H. Zhao, Preparation of titania nanotubes and their environmental applications as electrode, *Environ. Sci. Technol.*, 2005, **39**, 3770–3775.



140 S. Xu, J. Ng, X. Zhang, H. Bai and D. D. Sun, Adsorption and photocatalytic degradation of Acid Orange 7 over hydrothermally synthesized mesoporous  $\text{TiO}_2$  nanotube, *Colloids Surf, A*, 2011, **379**, 169–175.

141 J. Zhou and X. S. Zhao, in *Visible-Light-Responsive Titanium Dioxide Photocatalysts*, Springer, New York, NY, 2010, pp. 235–251, DOI: 10.1007/978-0-387-48444-0\_10.

142 J. Wang, B. Huang, Z. Wang, X. Qin and X. Zhang, Synthesis and characterization of C, N-codoped  $\text{TiO}_2$  nanotubes/nanorods with visible-light activity, *Rare Met.*, 2011, **30**, 161–165.

143 B. X. Lei, *et al.*, Ordered crystalline  $\text{TiO}_2$  nanotube arrays on transparent FTO glass for efficient dye-sensitized solar cells, *J. Phys. Chem. C*, 2010, **114**, 15228–15233.

144 S. Higashimoto, M. Sakiyama and M. Azuma, Photoelectrochemical properties of hybrid  $\text{WO}_3/\text{TiO}_2$  electrode. Effect of structures of  $\text{WO}_3$  on charge separation behavior, *Thin Solid Films*, 2006, **503**, 201–206.

145 A. Ghicov and P. Schmuki, Self-ordering electrochemistry: A review on growth and functionality of  $\text{TiO}_2$  nanotubes and other self-aligned  $\text{MO}_x$  structures, *Chem. Commun.*, 2009, 2791–2808.

146 K. Maeda, *et al.*, Photocatalytic overall water splitting promoted by two different cocatalysts for Hydrogen and Oxygen evolution under visible light, *Angew. Chem., Int. Ed.*, 2010, **49**, 4096–4099.

147 K. Shankar, G. K. Mor, A. Fitzgerald and C. A. Grimes, Cation effect on the electrochemical formation of very high aspect ratio  $\text{TiO}_2$  nanotube arrays in formamide-water mixtures, *J. Phys. Chem. C*, 2007, **111**, 21–26.

148 Y. Sun, K. Yan, G. Wang, W. Guo and T. Ma, Effect of Annealing Temperature on the Hydrogen Production of  $\text{TiO}_2$  Nanotube Arrays in a Two-Compartment Photoelectrochemical Cell, *J. Phys. Chem. C*, 2011, **115**, 12844–12849.

149 X. Kang and S. Chen, Photocatalytic reduction of methylene blue by  $\text{TiO}_2$  nanotube arrays: effects of  $\text{TiO}_2$  crystalline phase, *J. Mater. Sci.*, 2010, **45**, 2696–2702.

150 H. J. Oh, *et al.*, Synthesis of effective titania nanotubes for wastewater purification, *Appl. Catal., B*, 2008, **84**, 142–147.

151 P. Acevedo-Peña, J. E. Carrera-Crespo, F. González and I. González, Effect of heat treatment on the crystal phase composition, semiconducting properties and photoelectrocatalytic color removal efficiency of  $\text{TiO}_2$  nanotubes arrays, *Electrochim. Acta*, 2014, **140**, 564–571.

